

Collision Avoidance Operations for LEO Satellites Controlled by GSOC

S. Aida¹, M. Kirschner², M. Wermuth³ and R. Kiehling⁴

German Space Operations Center
DLR Oberpfaffenhofen
82234 Wessling, Germany

I. Introduction

The ever increasing population of objects in the near Earth environment has created growing concerns among satellite owners and control centers about the safety of their missions. The GSOC (German Space Operations Center) is currently building up an operational proximity monitoring and mitigation concept.

Contrary to locally operated satellites, high accurate orbital parameters are not available for the bulk of other space objects. Currently, the TLE (Two-Line Elements) catalogue maintained by the USSTRATCOM (US Strategic Command) constitutes the only publicly available and reasonably comprehensive orbit information. Despite evident deficiencies in the quality and timeliness of this information, it is currently a mandatory element for any operational proximity monitoring. The careful assessment of the TLE accuracy is therefore required to reveal the inherent modeling accuracy of the SGP4 analytical orbit model, as well as the orbit determination and orbit prediction accuracy for TLEs provided by USSTRATCOM.

Even after a realistic error analysis, the exclusive use of TLE data is insufficient for a proper planning and implementation of collision avoidance maneuvers. The orbit information of a possible jeopardizing object has to be refined in due time before a predicted proximity, if a predefined threshold of collision probability or safety distance is violated. To this end, the use of radar tracking is foreseen. The orbit refinement using radar tracking is necessary for a consolidated decision and implementation of an evasive maneuver.

Following a presentation of GSOC collision avoidance procedure for LEO (Low Earth Orbit) satellites, the paper will discuss the orbit accuracy as well as the improvement of the TLE orbit information by a radar tracking campaign. The orbit accuracy analysis is done by comparing corresponding orbit data with accurate orbit information from locally controlled space missions. The application to the collision risk monitoring system at GSOC is discussed hereafter, followed by the presentation of the monitoring system and the handling of close approaches.

II. Collision Avoidance Procedure at GSOC

GSOC has been implementing a collision avoidance system since 2008. The first version of the software for the close approach detection is running since January 2009 and operationally available since November 2009. A monitoring is currently performed twice a day in an automated process, detecting close approaches of operational LEO satellites against nearly 15000 space objects listed in the TLE catalogue provided by USSTRATCOM.

In the current collision avoidance system at GSOC (Figure 1), the procedure consists of mainly 3 steps. First, the potential collision risk of the operational satellites is detected over 7 following days using a TLE catalogue as well as precise orbit data of the operational satellites. Detected close approach events are listed in a report file, if the distance to a jeopardizing object is smaller than the pre-defined distance thresholds. The collision probability is also calculated for the potential close approach based on the method described in [1]. If the resulting collision probability exceeds the probability threshold, which is currently set to 10^{-4} , the collision risk is closely evaluated by analyzing the geometry at the time of the closest approach, prediction histories among others. In case a high collision risk is expected from the analysis, the orbit refinement using a radar tracking is foreseen as the second step. The accuracy of radar tracking was investigated in [2]. Finally, the close approach event is further analyzed based on the precise and latest orbit information, and a collision avoidance maneuver is planned if required.

¹ Space Flight Technology, saika.aida@dlr.de.

² Space Flight Technology, michael.kirschner@dlr.de.

³ Space Flight Technology, martin.wermuth@dlr.de.

⁴ Space Flight Technology, reinhard.kiehling@dlr.de.

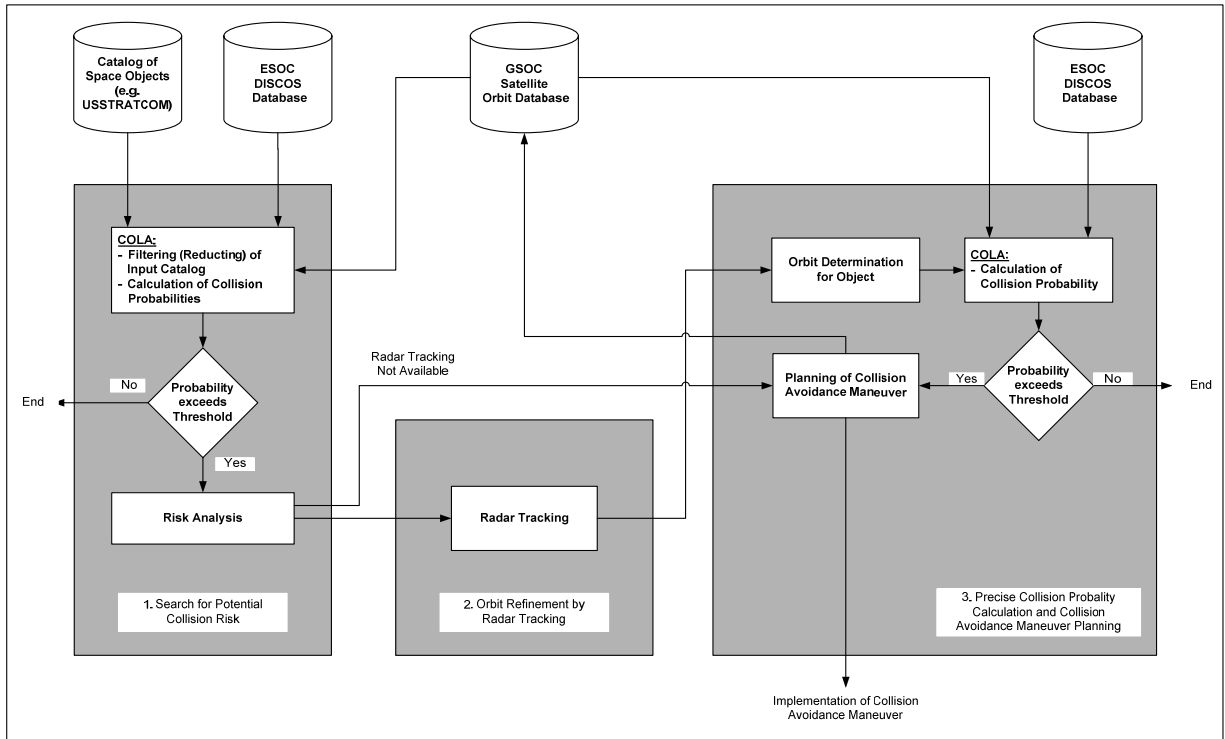


Figure 1 Collision Avoidance Procedure at GSOC

III. Analysis of Orbit Prediction Accuracy

In order to derive criteria for critical conjunctions an analysis for the OP (Orbit Prediction) accuracy was performed. First results have been given in [2].

Besides the large number of roughly 15000 catalogued objects in orbit, which requires proper search strategies for an efficient forecast of close approaches, users of the USSTRATCOM data have to cope with the limited accuracy of the provided orbit information, which is not publicly available. While an overly trust in the quality of the orbital data might result in an underestimation of the true collision risk, a pessimistic accuracy assessment would result in frequent close approach warnings. Any unnecessary collision avoidance maneuver would, in turn, notably increase the mission cost in terms of fuel consumption, reduced operational lifetime, man power and science data losses. Due to these constraints it is of advantage to have a good knowledge of the precision of the TLE orbits.

To investigate the TLE precision, model differences between the analytical SGP4 propagation and the numerical orbit propagation as well as propagation errors of ephemerides generated from USSTRATCOM TLEs and those generated by numerical orbit propagation were analyzed. The precise orbits of locally operated satellites CHAMP, GRACE-1, and TerraSAR-X (at an altitude of 270-430 km, 460-500 km and 510 km respectively) could be used to perform this analysis.

The well established OD (Orbit Determination) and OP software ODEM (Orbit Determination for Extended Maneuvers) was used to generate ephemerides based on numerical propagation. The OD inside ODEM is formulated as a sequential non-linear least-squares problem based on Givens rotations and the OP is based on a standard numerical integration method for initial value problems. In particular an Adams-Basforth-Moulton method for numerical integration of ordinary differential equations is adopted. This method employs variable order and step-size and is particularly suited for tasks like the prediction of satellite orbits. The numerical orbit propagator is using a comprehensive model for the acceleration of an Earth orbiting spacecraft under the influence of gravitational and non-gravitational forces.

The ‘real orbit’ as reference was generated by the software modules POSFIT or RDOD, which are part of the GHOST (GPS High Precision Orbit Determination Software Tool) package developed by GSOC/DLR. POSFIT performs a reduced dynamic orbit determination from a given a priori orbit. It estimates initial conditions, dynamical model parameters and empirical accelerations in a least squares fit. In addition, RDOD uses raw GPS measurements

as observations for a precise orbit determination (POD). The position accuracy of the orbits based on POSFIT and POD is better than 2 m and 10 cm, respectively.

A. Orbit Model

The differences between the two distinct orbit models, the analytical SGP4 and the numerical orbit propagator, were analyzed. The numerical orbit propagator was used to generate osculating ephemeris data, which served as measurement data for a SGP4 based OD. In other words the mean 2-line elements were determined from a best fit to the generated osculating trajectory. Details of this analysis are described in [2].

The analysis was performed in two steps, where at first the mean 2-line elements were determined for fit periods of 1 to 7 days. In the second step the generated TLEs were used to propagate the orbit over up to 7 days.

For satellites operating in LEO, the atmosphere has an important influence on the evolution of an orbit. The atmospheric density itself is directly depending on the solar activity, which can fluctuate dramatically within a few days. To avoid an influence of these fluctuations, constant solar activity parameters were used for the analysis.

One main outcome of the fitting analysis was that the RMS (Root Mean Square) errors in radial, along-track and normal direction are relatively constant for the different fit periods. An example of these errors is shown in Figure 2, which reflects clearly the model differences.

The main result of the propagation comparison was that a TLE fit should cover at least 2 days, otherwise the propagation of such a TLE orbit over more than 1 day makes no sense, as the error grows dramatically. Another important result was that the propagation error increases with the influence of the atmosphere, i.e. for lower altitudes or higher solar activity.

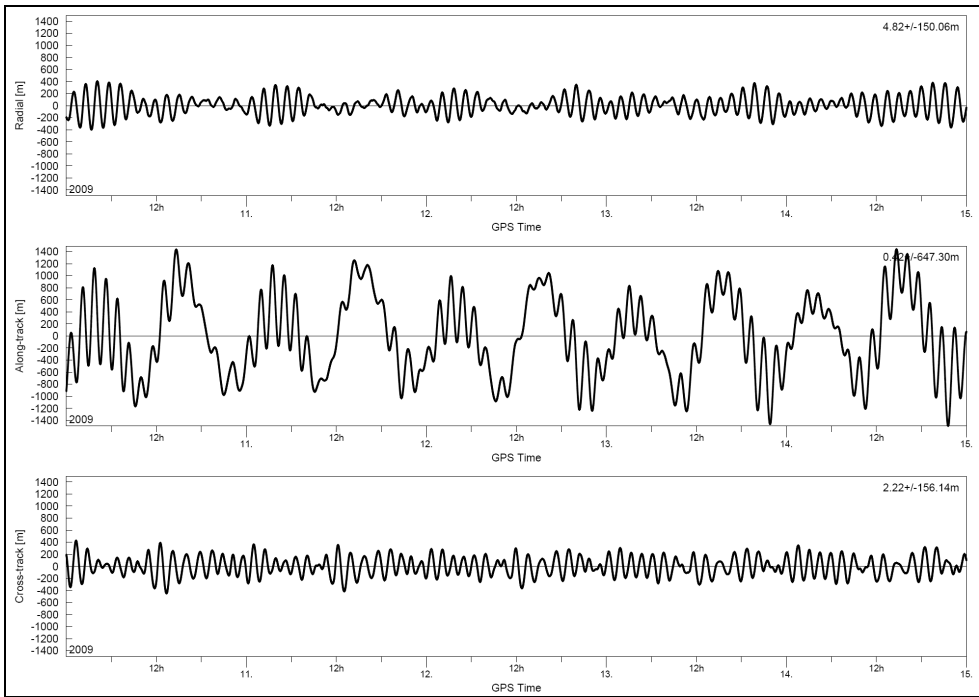


Figure 2 RTN (radial/along-track/normal) Error of a 5-day-TLE-fit w.r.t. Numerically Propagated Orbit

B. Influence of Solar Flux and Altitude on TLE Orbit Propagation Accuracy

In the analysis of [2], errors of the propagated TLEs from POD orbits were investigated during a period of low solar flux. On the other hand, the analysis of the TLE fit against osculating orbit ephemerides showed that the solar activity can have an important influence on the prediction error. The significant influence of the solar activity on the OP accuracy is also shown for the numerical propagation in [3]. As the solar activity is slowly increasing since end of 2009, it is also important now to know more in detail the influence of the solar activity on the orbit prediction. Therefore the orbit prediction accuracy analysis was extended to investigate the dependency of the prediction accuracy not only on the altitude but also on the solar flux, using orbit data for a long period. For two satellite

missions at GSOC, CHAMP and GRACE, GPS orbits are available during the whole bandwidth of the solar activity, since CHAMP was launched in 2000 and GRACE in 2002.

Likewise the analysis in [2], TLEs for each satellite were propagated to the corresponding POD epoch up to 7 days (forwards) using the SGP4 propagator. The resulting orbits were compared with the precise orbits of CHAMP (April 2001-July 2010), GRACE-1 (April 2002-July 2010) and also TerraSAR-X (July 2007-July 2010) which are available at an interval of 30 seconds.

Table 1 RTN Error of TLE Propagation (RMS in [m])

		1 day prop				4 days prop				7 days prop					
		Flux				Flux				Flux					
R	Altitude [km]	-90	90-140	140-190	190-	-90	90-140	140-190	190-	-90	90-140	140-190	190-		
	-300	309	208	275	225	-300	748	622	682	636	-300	2693	2498	3227	3446
	300-350	353	252	320	269	300-350	667	541	601	555	300-350	1007	812	1541	1761
	350-400	285	234	301	251	350-400	579	507	566	520	350-400	988	955	1684	1904
	400-450	351	305	214	163	400-450	559	491	451	405	400-450	835	780	764	983
	450-500	333	293	369	317	450-500	622	558	628	591	450-500	912	836	953	884
	500-	219	178	254	203	500-	330	267	337	299	500-	466	389	506	438
T	Altitude [km]	-90	90-140	140-190	190-	-90	90-140	140-190	190-	-90	90-140	140-190	190-		
	-300	2925	1721	2035	2256	-300	40669	45697	50981	57079	-300	168530	136560	168530	189108
	300-350	2963	1758	2073	2294	300-350	12159	17187	22471	28568	300-350	35184	38817	70787	91365
	350-400	1528	1564	1878	2099	350-400	14163	15652	20936	27034	350-400	45122	47606	79577	100154
	400-450	1396	1438	1348	1569	400-450	8572	10802	12476	18574	400-450	30609	36578	37855	58432
	450-500	1312	1358	2343	2476	450-500	3830	6799	10747	18224	450-500	8240	17694	34904	43721
	500-	1207	1254	2239	2372	500-	2519	5489	9436	16913	500-	5456	14910	32120	40937
N	Altitude [km]	-90	90-140	140-190	190-	-90	90-140	140-190	190-	-90	90-140	140-190	190-		
	-300	482	409	495	502	-300	575	477	514	530	-300	669	453	451	481
	300-350	375	302	388	395	300-350	431	334	370	386	300-350	490	274	272	302
	350-400	248	300	386	393	350-400	256	303	340	356	350-400	283	320	318	348
	400-450	338	347	375	383	400-450	334	323	359	375	400-450	338	310	357	387
	450-500	324	290	401	367	450-500	358	289	393	368	450-500	402	309	390	401
	500-	418	383	494	461	500-	461	392	496	470	500-	499	406	486	497

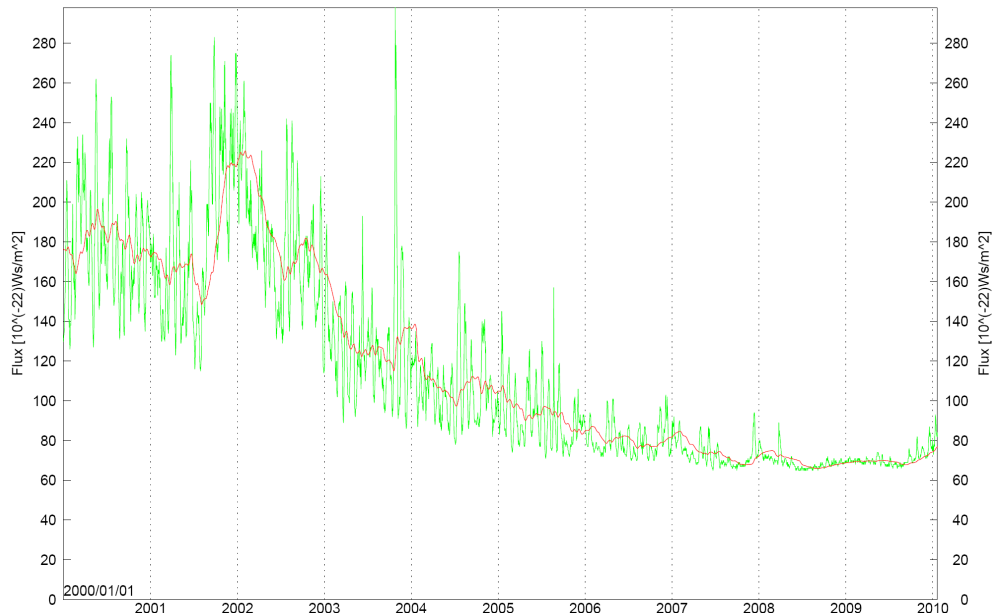


Figure 3 Solar Flux History as of January 2010

RMS errors sorted by the altitude and the solar flux at each POD epoch are shown in Table 1. Since they were not enough available data to cover all the altitude-flux sets, some RMS errors were substituted with the estimated value using linear extrapolation just to see the tendency of the error growth at the wider range of the altitude-flux set. The missing data was estimated from at least 3 surrounding cells in a 2×2 square data set, using the value at the intersection point of the two diagonals (Figure 4). When more than one square data set exists, the average from each square data was taken. This process was continued until all possible data are filled. In Table 1, such extrapolated data are distinguished from the statistical results by the dark pattern.

As a whole, the RMS errors of the along-track and radial components become larger at lower altitudes and also at higher solar flux periods and grows exponentially for longer prediction time. As shown in Figure 3, fluctuation of the solar flux is much larger during the higher flux period compared to the lower one. Due to this behavior and since the solar flux has a severe influence on the atmospheric density, the along track and also radial prediction errors are expected to become larger when the solar flux is higher and also when the altitude is lower. As for the RMS error of the normal component, there is no distinct dependency on the solar flux and the altitude, but the error grows gradually with the propagation length.

C. Influence of Solar Flux and Altitude on Numerical Orbit Propagation Accuracy

As done in the TLE analysis, the orbit prediction error was analyzed as well for the numerical propagation using the orbit database of CHAMP, GRACE-1 and TerraSAR-X. The orbits were propagated up to 7 days with the ODEM tool, and compared with the same precise orbits as used in B. For the numerical propagation, the predicted solar flux at the epoch of the database was used.

Table 2 RTN Error of Numerical Propagation (RMS in [m])

		1 day prop				4 days prop				7 days prop						
		Flux				Flux				Flux						
		-90	90-140	140-190	190-	-90	90-140	140-190	190-	-90	90-140	140-190	190-			
R	-300	19	22	23	25	-300	223	248	238	263	-300	1505	1681	3514	3430	
	300-350	5	7	9	11	300-350	36	62	51	77	300-350	125	301	2133	2050	
	350-400	8	10	12	14	350-400	43	69	58	84	350-400	282	458	2290	2207	
	400-450	6	7	8	10	400-450	24	40	46	71	400-450	67	170	204	120	
	450-500	5	6	6	8	450-500	12	19	25	50	450-500	22	52	210	127	
	500-	1	2	3	5	500-	8	14	20	46	500-	3	34	192	108	
T	-90	90-140	140-190	190-	-90	90-140	140-190	190-	-90	90-140	140-190	190-	-90	90-140	140-190	190-
	-300	1204	1390	1449	1584	-300	28388	30919	28833	31719	-300	97621	103106	134988	139301	
	300-350	278	463	522	657	300-350	7244	9775	7689	10575	300-350	24695	30179	62062	66375	
	350-400	530	668	727	862	350-400	10199	12730	10643	13529	350-400	34994	40479	72361	76674	
	400-450	337	466	449	585	400-450	6747	9085	9697	12582	400-450	22520	28769	36506	40819	
	450-500	97	217	332	468	450-500	1652	3796	5988	8874	450-500	5382	12395	22299	26612	
N	500-	22	142	257	392	500-	376	2520	4712	7598	500-	951	7964	17868	22181	
	-90	90-140	140-190	190-	-90	90-140	140-190	190-	-90	90-140	140-190	190-	-90	90-140	140-190	190-
	-300	3	3	3	4	-300	10	10	10	11	-300	19	19	21	20	
	300-350	2	2	2	2	300-350	5	5	5	6	300-350	8	9	11	10	
	350-400	1	1	1	1	350-400	4	4	5	5	350-400	7	8	10	9	
	400-450	1	1	1	2	400-450	4	4	5	6	400-450	7	8	10	9	
A	450-500	6	6	5	6	450-500	14	14	10	11	450-500	23	24	17	16	
	500-	1	1	1	1	500-	4	4	1	1	500-	5	6	0	0	

The resulting RMS errors in Table 2 show again the dominant prediction error in the along-track direction. Comparable to the TLE analysis, the along-track and radial errors become larger at the lower altitude and at the higher solar flux period. The RMS error of the normal component doesn't show the clear dependency on the solar flux and the altitude, but the error grows gradually with the longer propagation. By propagating orbits using the well-modeled propagator, errors are small especially for the radial and normal components and also for the along-

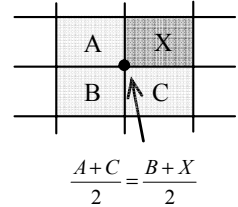


Figure 4 Data Extrapolation

track component during the short-term propagation. However, the longer propagation results in a bad orbit prediction especially in the along track direction. The reason could be a prediction error of the solar flux, which becomes larger at the higher solar flux period.

Table 3 shows the difference (in the mean and the standard deviation) between the predicted and the real solar flux values for different prediction periods. Flux data of the last 10 years (January 2001–July 2010) was taken for the analysis, where for each day a dedicated flux file was used containing 8-day-prediction data available at that day. These flux files are based on archived daily short-term predictions by ESOC. The results clearly show the growing prediction error for higher solar flux values, leading to the large along-track and radial error in the numerical propagation, even with the well-established model of the propagator.

Table 3 Solar Flux Prediction Error

		1 day pred.		4 day pred.		7 day pred.	
		Mean	1σ	Mean	1σ	Mean	1σ
<i>Flux</i>	-90	0.5	3.0	1.3	4.9	1.8	5.9
	90-140	1.4	11.6	3.5	16.8	5.3	19.2
	140-190	1.3	12.6	1.4	20.6	2.6	25.3
	190-	-6.4	21.7	-15.4	33.3	-23.6	39.1

D. Radar Tracking

As shown in [2] the TLE orbit accuracy can be improved by a radar tracking campaign for the encountering object to the quality of the OD accuracy based on GPS navigation solution data. The main objective of such a campaign is the enormous reduction of the radial uncertainty by a factor of 10-30, which can lead to a reduction of the number of collision avoidance maneuvers.

IV. Application to Collision Avoidance System

The current GSOC software for the close approach detection is daily running, which performs a prediction of proximity events for operational satellites over the 7 following days.

In the current process, TLE propagation errors obtained in the analysis of [2] are used to generate the covariance matrix of space objects in the relevant altitude range. Since these orbit uncertainties were obtained based on the orbit data during the low solar activity period, they are expected to become worse when the solar activity gets higher as shown in III-B. Therefore propagation errors in Table 1 will be further implemented to provide covariance information of space objects at the corresponding solar flux as well as altitude. For operational satellites, the numerical propagation errors are available as shown in Table 2. They can be also applied as covariance information instead of propagating an initial covariance matrix, which could result in a too optimistic estimation orbit uncertainties. The collision probability is then calculated from orbital states and covariance information at the estimated collision epoch.

It was also found out that the numerical propagation can result in a large orbit error for the long time prediction, although it is still better than the TLE propagation. However, the accuracy in the radial and along-track direction is much improved for the shorter period of prediction around 2-3 days, and even better around 1-1.5 days, which is the decision point for radar tracking and the maneuver planning respectively.

In case of a high collision risk, it is planned to perform radar tracking around 1.5 days before the predicted closest approach to refine the orbit information. Since the OD quality of a radar tracking data showed the same quality as that based on GPS navigation solution data, a radar tracking can be an effective way to detect the critical close approach and reduce unnecessary collision avoidance maneuvers.

V. Collision Risk Monitoring at GSOC

The collision risk of the operational satellites is daily monitored against space objects in the TLE catalogue. As of July in 2010, the monitoring includes 5 operational satellites in LEO, CHAMP (~ 260 km), GRACE-1 and 2 (~ 460 km), TerraSAR-X(~ 510 km), and lately launched TanDEM-X (~ 510 km). The upcoming events are listed in the report file when both distance thresholds, currently set to relative distance < 10 km and radial distance < 3 km, are violated. These thresholds were determined from the preliminary analysis of the TLE propagation errors. An example of the prediction results for TerraSAR-X is shown in Figure 5.

```

-----  

DLR                                         German Space Operations Center  

Program COLA run on 2009/11/27 17:09  

-----  

PREDICTION FROM: 2009/11/23 17:09:00.000  

      TO : 2009/11/30 17:09:00.000  

-----  

REL.DIST < 10.0 [km]  

RADIAL_DIST < 3.0 [km]  

-----  

TARGET_R : 2.60 [m]  

OBJECT_R : 2.00 [m] (Default)  

-----  

SatID Name          Days since     Time of approach    Max.Prob       Obj.R  

                                         Min.Range     Rel.Vel   OrbPl.Angl  

                                         [km]          [km/s]    [deg]  

                                         R           T           N  

                                         [km]         [km]        [km]  

                                         OrbArcDist TimFromNode DstFromNode  

                                         [km]          [sec]        [km]  

-----  

31698 TerraSAR-X      0.992 S:2009/11/27 05:39:07.180  8.46E-05      DEFAULT  

33801 COSMOS 2251 DEB  1.607 2009/11/27 05:39:07.837   0.360       15.193     169.80  

                           0.924 E:2009/11/27 05:39:08.495   -0.128      -0.026     -0.335  

                                         0.081       0.248      1.891

```

Figure 5 Results of Close Approach Prediction

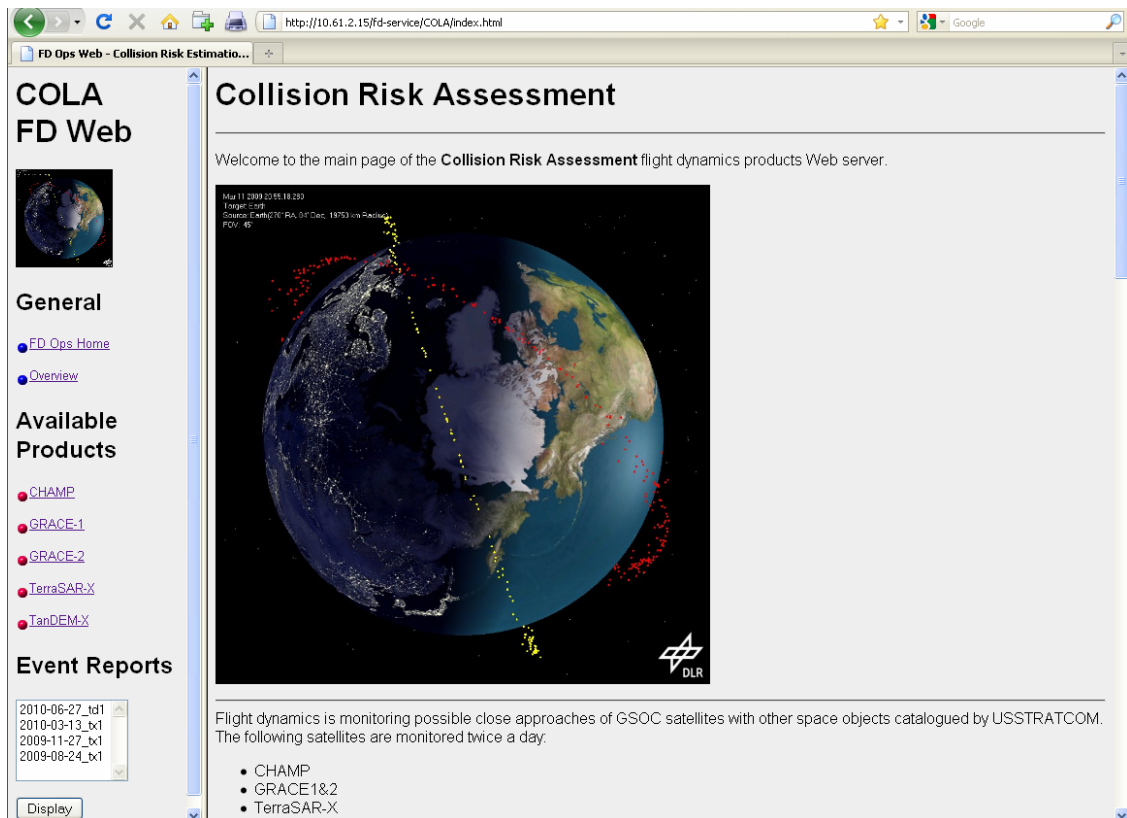


Figure 6 Snapshot of GSOC's Website for Collision Risk Assessment

In Figure 5, following the prediction epoch, distance thresholds and size information, close approach events are described along with the maximum probability and the close approach geometry. The important parameters for an assessment of the collision risk are the collision probability (“Max.Prob”), the radial distance between the two orbital arcs (“OrbArcDist”), which is the possible minimum distance between the two objects, the total distance (“Min.Range”) as well as the fly-by direction given by the angle between the two orbital planes (“OrbPl.Ang”). The estimated orbit uncertainty at the corresponding propagation time (“Days since”) is also considered for the risk assessment. R/T/N give the relative distances of the object in the local orbital frame relative to the own spacecraft (radial/tangential/normal). This report is updated twice a day using the latest orbit information.

The latest prediction report is available on the internal flight dynamics website, so that GSOC staff can share the information about the upcoming close approaches. The main page of the GSOC collision risk assessment is shown in Figure 6. By selecting a satellite on the left-hand side, a prediction report for the corresponding satellite is shown. Reports for the past critical events are also listed, containing the event summary, the collision probability history, and, if avoidance maneuvers were executed, details of the implemented maneuvers.

VI. Handling of Close Approach

If a maximum probability exceeds the current probability threshold of 10^{-4} , the event is analyzed closely to assess its criticality. When a critical approach is expected after the analysis, a radar tracking campaign is performed about 1.5 days before the time of the closest approach if available to refine orbit information of the encountering object. The collision risk is then assessed again using the refined and latest orbit information, and collision avoidance maneuvers are planned in case of a high collision risk. Even if a radar tracking is not available, prediction results are constantly updated using the latest orbit data until the final decision, which is done around 0.5-1.0 days before the close approach time.

A. Risk Analysis

In case the probability threshold is violated, the criticality of the event is assessed carefully by analyzing the collision probability, the close approach geometry and also the TLEs of the encountering object. Some tools for the event analysis have been developed, such as the 3D visualization, the geometry quick view and the history of relative positions using TLEs. Figure 7 is a snapshot of the visualization tool, where the satellite and the encountering objects are shown along with the combined covariance ellipsoid. Such tools are helpful for the better understanding of the close approach geometry and accordingly for the implementation of collision avoidance maneuvers. The TLE history has also to be analyzed, since the orbit information of each TLE is not always consistent. Therefore the past TLEs of the encountering object are assessed along with the latest one and used for computation of the collision probability and the closest position.

B. Maneuver Planning

For the planning a collision avoidance maneuver, one of the following strategies is normally considered: a change of the execution epoch or the size of an upcoming regular maneuver, or the implementation of an additional maneuver reducing the collision probability. The former is more preferable in the fuel consumption and operational aspects, but its availability depends on the timing of the planned maneuver. If any change of the regular maneuver is not possible, the latter maneuver planning strategy is applied to increase the relative distance mostly in the radial direction, considering the mission constraints of the satellite. In addition, another maneuver is often required to come back to the nominal orbit.

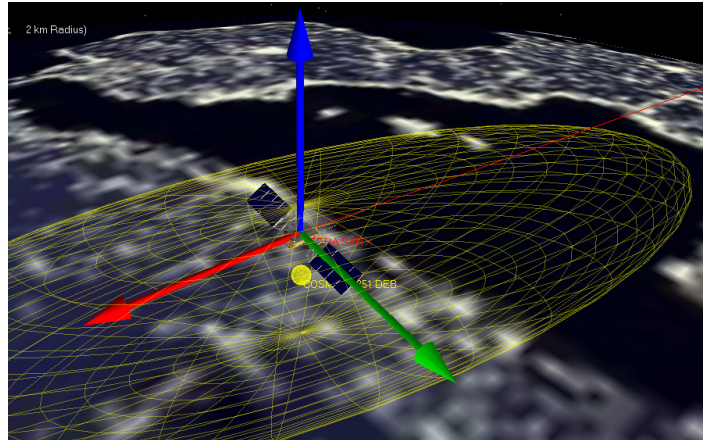


Figure 7 3D Visualization

As of July 2010, TerraSAR-X had 2 maneuver events in the nearly one year operation since the first record in the end of August 2009. In the first event, the avoidance maneuvers were decided based only on the warning from JSpOC (Joint Space Operations Center), resulting in the correction of the regular maneuver. In the second case, the maneuvers were decided based on the daily prediction using TLEs of the jeopardizing object, and collision avoidance maneuvers were planned as described in the following section. No radar tracking campaign was performed for both events.

C. Collision Avoidance Maneuver for TerraSAR-X

On November 27 2009, TerraSAR-X had a close approach against a Cosmos 2251 debris, which resulted in the first collision avoidance maneuver since the operational collision monitoring system started in November 2009. As shown in Table 4, the distance of the two orbital arcs was about 80 m, and all components of the relative position were within the estimated orbit uncertainty of the encountering object, which were ~ 0.25 km in radial, ~ 1.70 km in along-track, and ~ 0.45 km in normal direction. The collision probability history is shown in Figure 8, where the probability was approaching the threshold of 10^{-4} . Although it was once lowered 1.5 day before the time of the closest approach, the latest prediction showed the close probability again. Therefore an avoidance maneuver was planned to enlarge the radial distance by nearly 250 m. Two maneuvers were performed half an orbit before and after the closest approach in the along-track direction. The first maneuver was for the altitude increase, and the second one was for the altitude decrease, which was necessary to come back to the nominal orbit, and each maneuver was about 8 cm/s. The collision probability after the maneuver is also shown in Figure 8, where the probability was lowered from the threshold.

Table 4 TerraSAR-X Close Approach

Object		COSMOS 2251 DEB (ID 33801)
Object size	[m]	Unknown (RCS 0.037)
Time of the closest approach	[UTC]	2009/11/27 05:39:07.837
Min. distance	[km]	0.360
Relative position	[km]	-0.128, -0.026, -0.035
Orbital arc distance	[km]	0.081
Relative velocity	[km/s]	15.2

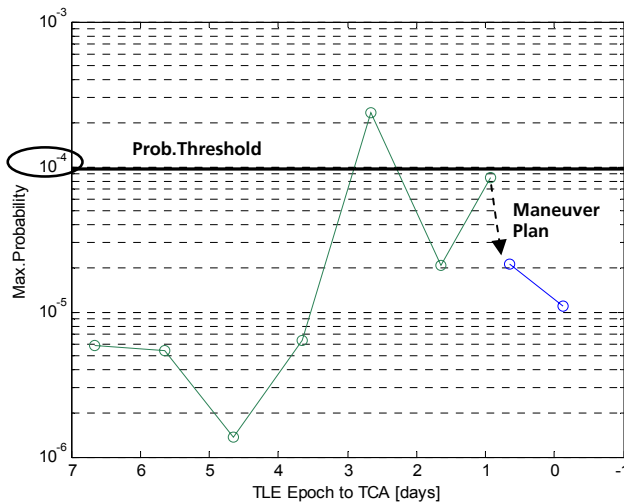


Figure 8 Probability History

VII. Conclusion

At GSOC, the collision avoidance system is operationally available since November 2009. The monitoring is currently running twice a day in an automated process, detecting close approaches of LEO satellites operated at GSOC against space objects in the TLE catalogue provided by USSTRATCOM.

For the proper collision risk assessment, the orbit precision and the TLE orbit refinement by a radar tracking campaign were discussed. In the orbit precision analysis, the SGP4 and numerical propagation were compared with POD orbits, and the dependency of the RMS error on the solar flux as well as the altitude was shown according to the orbit propagation length. The application of these results into the collision avoidance system at GSOC was addressed and the collision risk monitoring as well as the close approach event handling was presented.

References

- [1] Klinkrad, H., *Space Debris Model and Risk Analysis*, Springer-Verlag, Berlin, 2006, Chapter 8.
- [2] Aida, S., Patzelt, T., Leushacke, L., Kirschner, M., Kiehling, R., “Monitoring and Mitigation of Close Proximities in Low Earth Orbit”, *21st International Symposium on Space Flight Dynamics*, Toulouse, 2009.
- [3] Arbinger, C., D’Amico, S., “Impact of Orbit Prediction Accuracy on Low Earth Remote Sensing Flight Dynamics Operations”, *18th International Symposium on Space Flight Dynamics*, Munich, Germany, 2004.